Hsp90 inhibition transiently activates Src kinase and promotes Src-dependent Akt and Erk activation

Fumitaka Koga*, Wanping Xu*, Tatiana S. Karpova†, James G. McNally†, Roland Baron‡, and Len Neckers*§

*Urologic Oncology Branch, Center for Cancer Research, National Cancer Institute, Building 10, Room 1-5940, Bethesda, MD 20892-1107; †Laboratory of Receptor Biology and Gene Expression, National Cancer Institute, Bethesda, MD 20892; and ‡Department of Orthopedics, Yale University School of Medicine, New Haven, CT 06510

Communicated by Sue Hengren Wickner, National Institutes of Health, Bethesda, MD, June 6, 2006 (received for review May 9, 2006)

Hsp90 plays an essential role in maintaining stability and activity of its clients, including oncogenic signaling proteins that regulate key signal transduction nodes. Hsp90 inhibitors interfere with diverse signaling pathways by destabilizing and attenuating activity of such proteins, and thus they exhibit antitumor activity. However, Hsp90 inhibition has recently been reported to activate Akt and Erk and potentiate Akt activation induced by insulin-like growth factor 1 and insulin, raising the concern that clinical use of Hsp90 inhibitors might promote tumor progression under certain circumstances. Here, we show that the prototypical Hsp90 inhibitor geldanamycin induces Akt and Erk activation that is independent of PTEN status and is mediated by transient activation of Src kinase. Activated Src phosphorylates Cbl, which recruits the p85 subunit of phosphatidylinositol 3-kinase, resulting in phosphatidylinositol 3-kinase activation and eventually the activation of Akt and Erk. We show that geldanamycin rapidly disrupts Src association with Hsp90, suggesting that Src activation results directly from dissociation of the chaperone. These data suggest that, under certain circumstances, dual inhibition of Hsp90 and Src may be warranted.

cancer | chaperone | geldanamycin

The molecular chaperone Hsp90 is constitutively expressed in mammalian cells and plays an essential role in facilitating the proper folding, maturation, and activity of its client proteins (1). Hsp90 associates with its client proteins in an ATP-dependent manner (2, 3). The naturally occurring anasamycin antibiotic geldanamycin (GA) specifically interferes with this association by occupying the ATP binding pocket of Hsp90 and dissociates client proteins from the chaperone, which results in their degradation by the ubiquitin-dependent proteasome pathway (4–6). Neoplastic cells frequently overexpress Hsp90, and a number of oncogenic signaling proteins depend on Hsp90 function, including ErbB2, Src family kinases, Akt, Raf-1, mutated p53, and hypoxia-inducible factor 1α (1). GA and other Hsp90 inhibitors interfere with multiple signal transduction pathways by destabilizing these signaling proteins, thus exhibiting antitumor activity in diverse neoplasms (1). Clinically, the GA-derivative 17-allylamino-17-demethoxygeldanamycin has progressed to evaluation in multiple phase-II trials.

Although inhibition of Hsp90 function has been thought to only attenuate activity of its client protein kinases, GA was recently reported to rapidly but transiently activate the dsRNA-dependent kinase PKR in HeLa cells (7) and Akt kinase in myoblast cells (8) and to potentiate Akt activation induced by insulin-like growth factor and insulin in neuroblastoma and human embryonic kidney 293 cells (9). In addition, GA transiently activates Erk kinase, which is not an Hsp90 client, in HeLa cells (7). In the case of PKR, activation of its kinase activity is most likely caused by GA-induced rapid dissociation of Hsp90 (7). However, because Hsp90 inhibitors do not affect chaperone interaction with either Akt (8, 9) or Erk, how Hsp90 inhibition enhances the activity of these kinases remains undetermined. Given the potential contributions of activated Akt and Erk to the progression and drug resistance of numerous cancers, it is imperative to understand the molecular basis of this phenomenon. Here, we report that the Hsp90 inhibitor GA stimulates Akt and Erk via transient activation of Src kinase and that Src activation is likely caused by its dissociation from Hsp90.

Results

GA Transiently Activates Akt and Erk via Phosphatidylinositol 3-Kinase (PI3-Kinase). Hsp90 functions to stabilize Akt kinase (10, 11). However, when we treated T24 bladder carcinoma cells with 1 μM GA, we observed a rapid and transient, but reproducible, increase in Akt phosphorylation on Ser-473, an indicator of Akt activity, at a time when total Akt protein levels remained unchanged (15 min to 4 h after treatment). Akt phosphorylation increased >2-fold by 30 min of treatment, and then gradually decreased, in parallel with the decrease in total Akt protein levels at later time points (Fig. 1*A*). Because the lack of functional PTEN in T24 cells (12) could contribute to this phenotype, we examined the occurrence of this phenomenon in MCF7 breast cancer cells, which express functional PTEN (13). As was the case in T24 cells, brief exposure of MCF7 cells to GA led to increased phosphorylation of Akt on Ser-473 (Fig. 2*D*).

To determine whether GA activates Akt directly or via upstream effectors, we pretreated T24 cells with LY294002, an inhibitor of PI3-kinase, the major mediator of Akt phosphorylation. LY294002 completely inhibited GA-induced Akt phosphorylation (Fig. 1*B*), indicating that, most likely, GA activates Akt at the level of or upstream of PI3-kinase. GA-induced Erk phosphorylation was also PI3-kinase-dependent (Fig. 1*B*), but it was attenuated more rapidly than that of Akt, although the total Erk protein level was not affected (Fig. 1*A*). Erk could be activated as a result of crosstalk between PI3-kinase and the Raf/MEK/Erk pathway (14, 15), whereas its rapid inactivation could be the net result of negative feedback of activated Akt on Raf (15, 16) plus a direct inhibition of Raf by GA (17). These experiments do not rule out a possible contribution of (downstream) feedback loops to GA-induced activation of either Akt or Erk.

GA Activates Src Kinase. Src kinase is involved in coordinating ligand-induced signaling via receptor tyrosine kinases with downstream signaling pathways, and it acts upstream of PI3-kinase (18, 19). To examine the possible involvement of Src in GA-induced PI3-kinase activation, we first determined whether GA activates Src. We found that GA increased Src phosphorylation on Tyr-418, an indicator of Src activation. The increase reached a peak of 1.7-fold at 30 min and subsequently declined, going below the basal level by 120 min (Fig. 2*A*). During this time, there was no discernible change in Src protein level.

Conflict of interest statement: No conflicts declared.

Abbreviations: CFP, cyan fluorescent protein; GA, geldanamycin; PI3-kinase, phosphatidylinositol 3-kinase; SH, Src homology; siRNA, small interfering RNA; YFP, yellow fluorescent protein.

§To whom correspondence should be addressed. E-mail: neckersl@mail.nih.gov.

www.pnas.org/cgi/doi/10.1073/pnas.0604705103

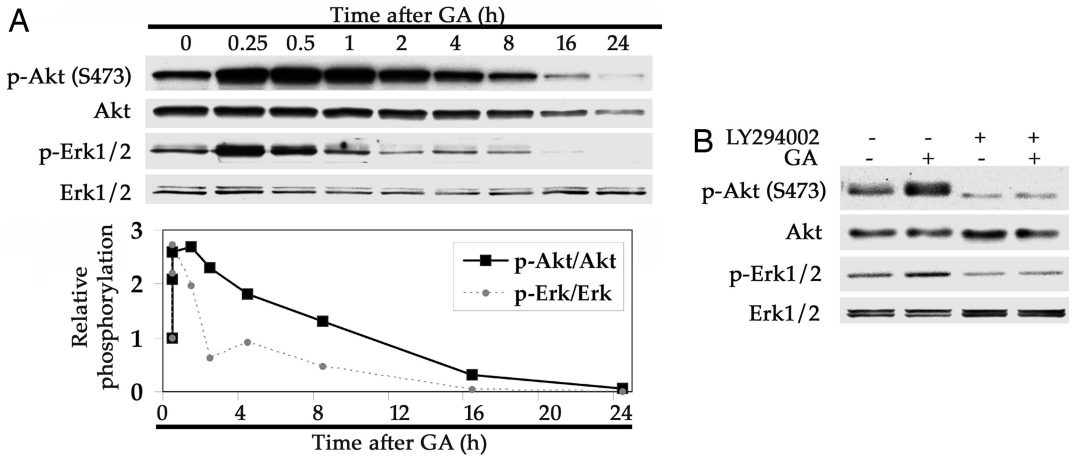

Fig. 1. Transient activation of Akt and Erk by GA requires PI3-kinase. (*A*) GA transiently activates Akt and Erk. T24 cells were treated with 1 μM GA for the indicated times. Phosphorylation and protein levels of Akt and Erk in total cell lysate were detected by Western blot using specific antibodies. Ratios of phosphor-Akt and phosphor-Erk to total Akt and total Erk, respectively, are graphically depicted as a function of time after GA addition. (*B*) GA-induced Akt and Erk activation depends on PI3-kinase activity. T24 cells were treated with 50 μM LY294002 or DMSO for 1 h followed by treatment with 1 μM GA or DMSO for 30 min. Phosphorylation and protein levels were detected as described above.

Importantly, GA-induced Src activation was temporally correlated to Akt activation. Further, the magnitude and duration of Src activation induced by GA was similar to that induced by hepatocyte growth factor (data not shown). Next, we examined the role of Src in GA-induced Akt and Erk activation. The Src kinase inhibitor PP1 completely abolished the ability of GA to activate both Akt and Erk in T24 cells (Fig. 2*B*). In contrast, treatment with LY294002 failed to abrogate GA-induced Src

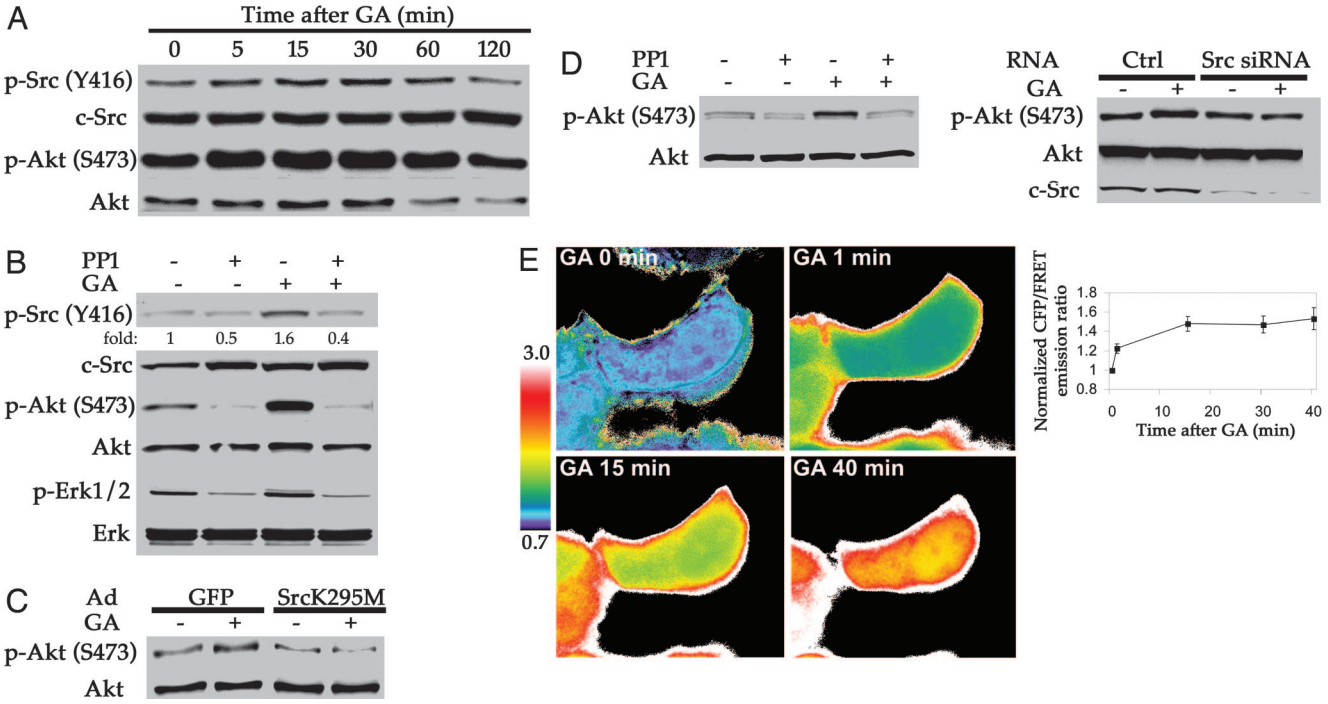

Fig. 2. GA activates Src, and GA-induced Akt and Erk activation are Src-dependent. (*A*) GA transiently increases phosphorylation of Src Y418 (Y416 in chicken). T24 cells were treated with 1 μM GA for the indicated times. Phosphorylation and protein levels of Src and Akt in total cell lysate were detected by Western blot. (*B*) Src inhibitor PP1 blocks GA-induced activation of Akt and Erk. T24 cells were pretreated with 10 μM PP1 or DMSO for 30 min and incubated with 1 μM GA or DMSO for 30 min. Phosphorylation and protein levels of Src, Akt, and Erk in total cell lysate were detected by Western blot. (*C*) Kinase-dead Src, SrcK295M, abrogates GA-induced Akt activation. T24 cells infected with an adenoviral vector carrying GFP or SrcK295M at 200 multiplicities of infection were treated with 1 μM GA for 30 min. Akt phosphorylation and protein levels in cell lysates were determined by Western blot. (*D*) PP1 (*Left*) and c-Src siRNA (*Right*) abolish GA-induced Akt activation in MCF7 cells. (*Left*) MCF7 cells were pretreated with 10 μM PP1 or DMSO for 30 min and incubated with 1 μM GA or DMSO for 30 min. (*Right*) MCF7 cells transfected with control RNA or c-Src siRNA were treated with 1 μM GA or DMSO for 30 min. Phosphorylation status and total protein levels of Akt and Src were detected by Western blot. (*E*) GA induces Src activation in live cells. MCF7 cells expressing the FRET-based Src reporter were treated with 1 μM GA, and images collected after the indicated times were analyzed. Representative time-dependent CFP/YFP (FRET) emission ratio images of a single cell in response to GA (*Left* and Movies 1 and 2) and the time course of the CFP/YFP (FRET) emission ratio of the entire field of 10 cells, normalized to the control data, in response to GA (*Right*; mean ± SEM of 10 cells in a field) are shown.

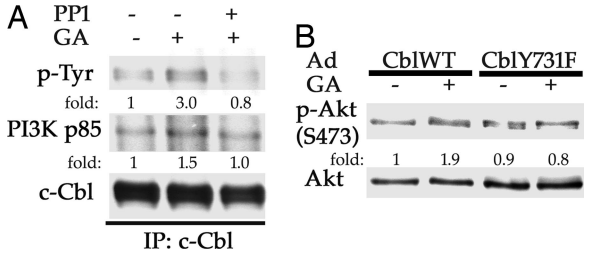

Fig. 3. Cbl mediates GA-induced, Src-dependent PI3-kinase activation. (*A*) GA induces Cbl tyrosine phosphorylation and PI3-kinase p85 binding to Cbl in an Src-dependent manner. Cbl was immunoprecipitated from T24 cells treated as shown with 10 μM PP1 for 30 min followed by 1 μM GA for 30 min, and the blot was probed with indicated antibodies. (*B*) Cbl Y731 mediates GA-induced Akt activation. T24 cells infected with an adenovirus carrying WT Cbl (CblWT) or Cbl with Y731F mutation (CblY731F) at 200 multiplicities of infection were treated with 1 μM GA for 30 min. Akt phosphorylation and protein levels were detected by Western blot using total cell lysates.

activation (data not shown), suggesting that Src is the proximal effector of this rapid cellular response to GA. To further confirm the importance of Src in this phenomenon, we infected T24 cells with an adenovirus expressing kinase-dead Src (SrcK295M) (20). Kinase-dead Src protein was expressed at as much as 5-fold the level of endogeneous Src (in cells infected at a multiplicity of infection of 200; see Fig. 5, which is published as supporting information on the PNAS web site). Consistent with our previous data, overexpression of SrcK295M abolished GA-induced Akt activation (Fig. 2*C*). Finally, both pharmacologic inhibition of Src with the small molecule inhibitor PP1 and molecular knockdown of the protein with c-Src small interfering RNA (siRNA) abolished the ability of GA to activate Akt in MCF7 cells (Fig. 2*D*).

Next, to confirm occurrence of GA-induced activation of Src kinase in live cells, we transfected MCF7 cells with a FRET-based Src reporter that has been characterized in detail (21). Briefly, this construct is composed of cyan fluorescent protein (CFP) and yellow fluorescent protein (YFP), separated by an Src homology (SH) 2 domain, a flexible linker, and an Src-specific phosphorylation site. In its unphosphorylated state, the reporter's conformation allows juxtaposition of CFP and YFP domains so that excitation of CFP results in energy transfer to YFP, yielding emission from YFP (high FRET). Src phosphorylation alters the conformation of the reporter, separating YFP and CFP domains and decreasing the FRET. Thus, an increase in the measured ratio of CFP emission intensity to YFP (FRET) intensity is a sensitive indicator of real-time Src activity in live cells. In MCF7 cells transiently transfected with the Src reporter, GA increased the CFP/YFP (FRET) ratio, particularly in the cell periphery, to a similar degree and with kinetics consistent with our earlier observations (Fig. 2*E*; also see Movies 1 and 2, which are published as supporting information on the PNAS web site), confirming that Src kinase is indeed rapidly activated by GA in live cells. Taken together, these data suggest that GA initially activates Src kinase followed by Src-dependent activation of Akt and Erk.

Cbl Mediates GA-Induced PI3-Kinase Activation Downstream of Src. Cbl, an E3 ubiquitin ligase and adaptor protein, not only down-regulates several tyrosine kinases but also serves as an adaptor to mediate their downstream signaling (22). Of the 22 tyrosine residues in Cbl, phosphorylation of Tyr-731 promotes binding of the p85 subunit of PI3-kinase, which leads to activation of PI3-kinase p110 (23, 24). Tyr-731 is an Src phosphorylation site (22), and the Src/Cbl/PI3-kinase pathway is essential for bone resorption by osteoclasts (20, 25). We therefore determined the possible involvement of Cbl in GA-induced PI3-kinase

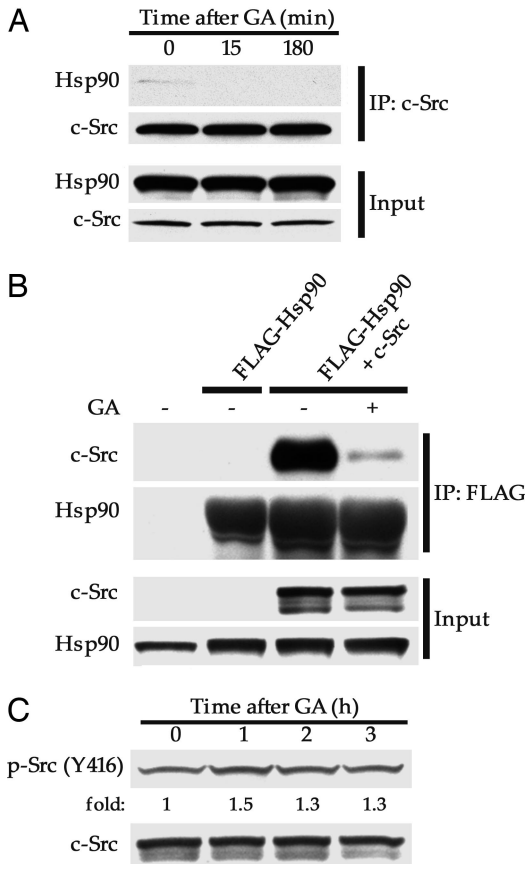

Fig. 4. GA induces concurrent release of Src from Hsp90 and activation of the kinase. (*A*) Endogenous Src was immunoprecipitated from T24 cells treated with 1 μM GA for the indicated times, and the blot was probed for Hsp90 and c-Src. (*B*) FLAG-Hsp90 was immunoprecipitated from COS7 cells transiently cotransfected with FLAG-Hsp90 and c-Src, and the blot was probed for Hsp90 and c-Src. Before lysis, some cells were exposed to 1 μM GA for 1 h. (*C*) GA induces activation of exogenous Src. COS7 cells transfected with WT Src were treated with 1 μM GA for the indicated times. Src phosphorylation at Y416 and total Src protein were determined by Western blot.

activation downstream of Src. We found that GA elevated tyrosine phophorylation of Cbl in an Src-dependent manner, and that this was accompanied by increased Cbl/PI3-kinase p85 association (Fig. 3*A*). Furthermore, adenovirus-mediated overexpression of a mutant Cbl construct (CblY731F), which is incapable of recruiting p85 (20), abolished GA-induced Akt activation, whereas overexpression of WT Cbl did not (Fig. 3*B*). These data support the hypothesis that Cbl is an essential mediator of GA-induced, Src-dependent PI3-kinase activation.

GA Disrupts Src Association with Hsp90. Because activation of the Hsp90 client kinase PKR by GA occurs subsequent to drug-induced dissociation of the chaperone (7), we investigated whether Src activation after GA similarly depended on release of the kinase from Hsp90. In a first experiment, we immunoprecipitated endogenous Src from T24 cells exposed briefly to GA and probed resultant blots for coprecipitated Hsp90. Although difficult to observe, Hsp90 association with a portion of cellular Src was detectable. However, within 15 min of GA addition to the cells, Hsp90 could no longer be visualized in Src immunoprecipitates (Fig. 4*A*). To confirm this result, we transiently coexpressed FLAG-Hsp90 and c-Src in COS7 cells. After immunoprecipitating protein lysates with anti-FLAG antibody, we probed resultant blots for c-Src. In untreated cells, coprecipitated Src was readily observable. However, within 1 h of

treating cells with GA the amount of Src coprecipitating with FLAG-Hsp90 was markedly reduced, although the total cellular Src level was only minimally impacted (Fig. 4*B*). At this same time point we detected a 50% increase in Src activity (compared with untreated cells) as measured by the degree of Src Tyr-418 phosphorylation (Fig. 4*C*).

Discussion

We observed in this study that brief treatment with the Hsp90 inhibitor GA activated both Akt and Erk in human cancer cells, confirming earlier reports (7, 8). We showed that both Akt and Erk activation by GA require PI3-kinase activity but are independent of cellular PTEN status. Finally, we clearly demonstrated that GA-induced Src activation accounts for these processes, in part by phosphorylation of Cbl to serve as an adaptor protein that recruits the p85 subunit of PI3-kinase, thus providing a molecular mechanism for these observations. Although the mechanism by which GA stimulates Src is not yet proven, it is likely to depend on GA-induced loss of Hsp90 binding. Similar pharmacologic disruption of Hsp90 binding to PKR kinase coincides with its activation (7), and a transient increase in activity of the Hsp90 client ErbB2 after Hsp90 inhibitor-dependent dissociation of the chaperone has recently been reported (26). Thus, although client protein destabilization is likely to remain the predominant outcome of Hsp90 inhibition, it is important to consider that a previously unappreciated, albeit transient consequence of this process may be selective activation of clients.

Although Hsp90 is required for Src maturation (27), association of endogenous mature c-Src with Hsp90 is difficult to detect (28). Indeed, we found only a small amount of Hsp90 to coprecipitate with Src in T24 cells. An explanation of this apparent paradox may be found in recent studies detailing the complex structural alterations involved in the process of Src activation. Inactive Src exists in a clamped configuration in which the SH2 domain interacts with the C-terminal phospho-Tyr-529 residue, whereas the SH3 domain covers the kinase domain, sterically obstructing access to the recently identified Hsp90 binding loop (29, 30). In addition to dephosphorylation of Tyr-529, interaction with SH2 and/or SH3 ligands primes Src for activation by relaxing this inhibitory conformation and allowing the kinase to be fully activated by phosphorylation of Tyr-418 in the activation loop (31). We propose that this intermediate conformation, neither fully repressed nor fully active, interacts with Hsp90 via the now accessible chaperone binding loop (30), and that the subsequent release of Hsp90 permits efficient phosphorylation of Tyr-418. In this study, we observed a rapid increase in phosphorylation of Tyr-418 upon GA-induced release of Hsp90 from the small pool of Src protein with which it was associated. In addition, we observed that stimulation of integrin signaling with fibronectin, which recruits the SH3 domain of Src to the cytoplasmic domain of integrin and eventually leads to Src activation (32), promoted GA-sensitive Src interaction with Hsp90 (see Fig. 6, which is published as supporting information on the PNAS web site).

In the context of cancer, Hsp90 inhibitor-dependent Src activation, although subtle, may be of particular relevance. GA-induced Src activation appears to be a relatively common occurrence in human cells because this process was not only observed in T24 bladder cancer cells and MCF7 breast cancer cells, but also in human embryonic kidney 293 cells and two prostate cancer cell lines (LNCaP and PC-3; data not shown). Src activation is also likely involved in GA potentiation of insulin-like growth factor and insulin signaling (7, 9) because Src can directly phosphorylate insulin receptor substrate 1 (33) and insulin-like growth factor receptor (34). Although Src-dependent activation of Akt and Erk after GA is relatively short-lived, these data raise the concern that in certain contexts Hsp90 inhibition might favor tumor survival and/or progression. Indeed, a recent study reported that 17-allylamino-17-demethoxygeldanamycin (17-AAG) promotes formation of osteolytic lesions and bone metastases in a murine breast cancer model by potentiating osteoclastic bone resorption, even though the drug reduced tumor growth at the orthotopic site (35). Because Src is essential for osteoclast activity (20) and Src-induced activation of Akt and Erk promotes osteoclast survival (36, 37), 17-AAG-induced Src activation, as described in this study, may be responsible for the reported effects of 17-AAG on bone. If that is the case, coadministration of an Src inhibitor should prevent these unfavorable effects of Hsp90 inhibitors. These data suggest that a fuller appreciation of the complex role played by Hsp90 in regulating signal transduction pathways will better inform the clinical utility of Hsp90 inhibitors.

Materials and Methods

Antibodies and Reagents. Anti-c-Cbl antibody (C-15; Santa Cruz Biotechnology) was used for both immunoprecipitation and immunoblotting. Agarose conjugates of Src rabbit polyclonal (N-16; Santa Cruz Biotechnology) and FLAG mouse monoclonal antibodies (M2; Sigma) were used for immunoprecipitation. For immunoblotting, antibodies to phospho-Ser-473 Akt, Akt, phospho-Tyr-416 Src, c-Src, phospho-Erk1/2 (clone 10), Erk1/2, phospho-Tyr (Cell Signaling Technology, Beverly, MA), Hsp90 (SPA-835; StressGen Biotechnologies, Victoria, Canada), PI3-kinase p85 (Upstate Biotechnology, Lake Placid, NY), c-Src (clone 327; Calbiochem), and FLAG (M2; Sigma) were used. GA was obtained from the National Cancer Institute. LY294002 and PP1 were purchased from Cell Signaling Technology and Biomol (Plymouth Meeting, PA), respectively.

Cell Culture and Transfections. T24, MCF7, and COS7 cells (American Type Culture Collection) were grown in DMEM containing 10% FBS, 2 mM L-glutamine, and 10 mM Hepes (pH 7.5) at 37°C and 5% CO_2. Replication-deficient adenovirus carrying GFP, SrcK295M, myc-tagged WT Cbl (CblWT), and myc-tagged CblY731F were as described (20). T24 cells at 60% confluence were infected with these viruses at 200 multiplicities of infection in a minimal amount of serum-free DMEM for 24 h followed by a 24-h incubation in fresh serum-free DMEM. Expression of transfected genes was confirmed by observing GFP with a fluorescent microscope and immunoblotting with antibodies against avian Src or myc tag. For all of the viruses, infection efficiencies were ≈80% (see Fig. 5). Before every treatment with drugs, T24 cells were serum-starved for 24 h. MCF7 and COS7 cells were transfected with expression plasmids with FuGene reagent (Roche Molecular Biochemicals) according to the manufacturer's instructions. Src reporter construct (21) was a kind gift from R. Tsien (University of California, San Diego). WT c-Src cDNA in pUSEamp was obtained from Upstate Biotechnology. c-Src siRNA (SRC *SMARTpool* siRNA reagent; Upstate Biotechnology) was introduced in MCF7 cells by using siIMPORTER reagent (Upstate Biotechnology) according to the manufacturer's instructions. N-terminal fusion FLAG-Hsp90 plasmid was generated by ligating human Hsp90α cDNA (a kind gift from W. Houry, University of Toronto, Toronto) into the pcDNA3 vector (Invitrogen) in-frame with the FLAG epitope tag. Cells transfected with plasmids and siRNA were treated and lysed 48 and 72 h after transfection, respectively.

Immunoprecipitation and Immunoblotting. These experiments were performed as described (38). Briefly, cells were lysed by scraping in TNESV lysis buffer (50 mM Tris·HCl, pH 7.4/1% Nonidet P-40/1 mM EDTA/100 mM NaCl/1 mM Na_3VO_4) supplemented with Complete proteinase inhibitors (Roche Applied Science). For immunoprecipitation, TNMSV lysis buffer (50 mM

Tris·HCl, pH 7.4/0.1% Nonidet P-40/20 mM Na_2MoO_4/150 mM NaCl/1 mM Na_3VO_4) was used. Immunoprecipitates or cell lysates were resolved by 7.5% or 4–20% SDS/PAGE, transferred to nitrocellulose membrane, and probed with antibodies.

Microscopy and Image Analysis. MCF7 cells expressing the FRET-based Src reporter protein were maintained in phenol red-free DMEM containing 10% FBS, 2 mM L-glutamine, and 10 mM Hepes (pH 7.5) in LabTek II chambers (Nalge). Images were collected by using METAMORPH software (Molecular Devices) on an inverted Nikon TE300 microscope with a 60 × 1.4 NA objective (Nikon), Lambda 10–2 filter changer, and Cool Snap ES CCD camera (Roper Scientific, Trenton, NJ/Photometrics, Tucson, AZ). The stage was heated to 37°C with an ASI 400 stage heater (Nevtek, Burnsville, VA). Images were acquired with a JP4 Chroma CFP/YFP filter set including a 430/25-nm exciter filter, double dichroic beam splitter (86002v2bs), a 470/30-nm emission filter for CFP, and a 535/30-nm emission filter for YFP. Excitation light was attenuated with a neutral density filter with 32% light transmission. To correct for z-drift, at each time point we collected seven focal planes with 1-μm spacing and then selected the single focal plane with optimal focus. As a control, images of untreated cells were collected with the same time intervals as those of treated cells. CFP and YFP images were background-subtracted, and the CFP/YFP (FRET) ratio images were computed with METAMORPH software. From those images, the average intensity over time was measured for individual cells and normalized to the first time point. The averaged data for treated cells were normalized to the averaged control data. The cell images are presented in pseudocolor to highlight the changes in the ratio of CFP/YFP (FRET) fluorescence intensity over time. Because no increase in CFP emission was observed over the time course of the experiment (see Movie 2), an increased CFP/YFP (FRET) ratio reflects a reduction of the FRET signal.

1. Neckers, L. (2002) *Trends Mol. Med.* **8,** S55–S61.
2. Panaretou, B., Prodromou, C., Roe, S. M., O'Brien, R., Ladbury, J. E., Piper, P. W. & Pearl, L. H. (1998) *EMBO J.* **17,** 4829–4836.
3. Grenert, J. P., Johnson, B. D. & Toft, D. O. (1999) *J. Biol. Chem.* **274,** 17525–17533.
4. Schneider, C., Sepp-Lorenzino, L., Nimmesgern, E., Ouerfelli, O., Danishefsky, S., Rosen, N. & Hartl, F. U. (1996) *Proc. Natl. Acad. Sci. USA* **93,** 14536–14541.
5. Connell, P., Ballinger, C. A., Jiang, J., Wu, Y., Thompson, L. J., Hohfeld, J. & Patterson, C. (2001) *Nat. Cell Biol.* **3,** 93–96.
6. Xu, W., Marcu, M., Yuan, X., Mimnaugh, E., Patterson, C. & Neckers, L. (2002) *Proc. Natl. Acad. Sci. USA* **99,** 12847–12852.
7. Donze, O., Abbas-Terki, T. & Picard, D. (2001) *EMBO J.* **20,** 3771–3780.
8. Yun, B. G. & Matts, R. L. (2005) *Cell Signal* **17,** 1477–1485.
9. Meares, G. P., Zmijewska, A. A. & Jope, R. S. (2004) *FEBS Lett.* **574,** 181–186.
10. Sato, S., Fujita, N. & Tsuruo, T. (2000) *Proc. Natl. Acad. Sci. USA* **97,** 10832–10837.
11. Basso, A. D., Solit, D. B., Chiosis, G., Giri, B., Tsichlis, P. & Rosen, N. (2002) *J. Biol. Chem.* **277,** 39858–39866.
12. Tanaka, M., Koul, D., Davies, M. A., Liebert, M., Steck, P. A. & Grossman, H. B. (2000) *Oncogene* **19,** 5406–5412.
13. Patel, L., Pass, I., Coxon, P., Downes, C. P., Smith, S. A. & Macphee, C. H. (2001) *Curr. Biol.* **11,** 764–768.
14. Chaudhary, A., King, W. G., Mattaliano, M. D., Frost, J. A., Diaz, B., Morrison, D. K., Cobb, M. H., Marshall, M. S. & Brugge, J. S. (2000) *Curr. Biol.* **10,** 551–554.
15. Moelling, K., Schad, K., Bosse, M., Zimmermann, S. & Schweneker, M. (2002) *J. Biol. Chem.* **277,** 31099–31106.
16. Rommel, C., Clarke, B. A., Zimmermann, S., Nunez, L., Rossman, R., Reid, K., Moelling, K., Yancopoulos, G. D. & Glass, D. J. (1999) *Science* **286,** 1738–1741.
17. Schulte, T. W., Blagosklonny, M. V., Ingui, C. & Neckers, L. (1995) *J. Biol. Chem.* **270,** 24585–24588.
18. Mao, W., Irby, R., Coppola, D., Fu, L., Wloch, M., Turner, J., Yu, H., Garcia, R., Jove, R. & Yeatman, T. J. (1997) *Oncogene* **15,** 3083–3090.
19. Chan, P. C., Chen, Y. L., Cheng, C. H., Yu, K. C., Cary, L. A., Shu, K. H., Ho, W. L. & Chen, H. C. (2003) *J. Biol. Chem.* **278,** 44075–44082.
20. Miyazaki, T., Sanjay, A., Neff, L., Tanaka, S., Horne, W. C. & Baron, R. (2004) *J. Biol. Chem.* **279,** 17660–17666.
21. Wang, Y., Botvinick, E. L., Zhao, Y., Berns, M. W., Usami, S., Tsien, R. Y. & Chien, S. (2005) *Nature* **434,** 1040–1045.
22. Thien, C. B. & Langdon, W. Y. (2001) *Nat. Rev. Mol. Cell. Biol.* **2,** 294–307.
23. Hunter, S., Burton, E. A., Wu, S. C. & Anderson, S. M. (1999) *J. Biol. Chem.* **274,** 2097–2106.
24. Kassenbrock, C. K., Hunter, S., Garl, P., Johnson, G. L. & Anderson, S. M. (2002) *J. Biol. Chem.* **277,** 24967–24975.
25. Tanaka, S., Amling, M., Neff, L., Peyman, A., Uhlmann, E., Levy, J. B. & Baron, R. (1996) *Nature* **383,** 528–531.
26. Citri, A., Gan, J., Mosesson, Y., Vereb, G., Szollosi, J. & Yarden, Y. (2004) *EMBO Rep.* **5,** 1165–1170.
27. Xu, Y., Singer, M. A. & Lindquist, S. (1999) *Proc. Natl. Acad. Sci. USA* **96,** 109–114.
28. Bijlmakers, M. J. & Marsh, M. (2000) *Mol. Biol. Cell* **11,** 1585–1595.
29. Xu, W., Yuan, X., Xiang, Z., Mimnaugh, E., Marcu, M. & Neckers, L. (2005) *Nat. Struct. Mol. Biol.* **12,** 120–126.
30. Citri, A., Harari, D., Shochat, G., Ramakrishnan, P., Gan, J., Eisenstein, M., Kimchi, A., Wallach, D., Pietrokovski, S. & Yarden, Y. (2006) *J. Biol. Chem.* **281,** 14361–14369.
31. Harrison, S. C. (2003) *Cell* **112,** 737–740.
32. Arias-Salgado, E. G., Lizano, S., Sarkar, S., Brugge, J. S., Ginsberg, M. H. & Shattil, S. J. (2003) *Proc. Natl. Acad. Sci. USA* **100,** 13298–13302.
33. Lebrun, P., Mothe-Satney, I., Delahaye, L., Van Obberghen, E. & Baron, V. (1998) *J. Biol. Chem.* **273,** 32244–32253.
34. Peterson, J. E., Kulik, G., Jelinek, T., Reuter, C. W., Shannon, J. A. & Weber, M. J. (1996) *J. Biol. Chem.* **271,** 31562–31571.
35. Price, J. T., Quinn, J. M., Sims, N. A., Vieusseux, J., Waldeck, K., Docherty, S. E., Myers, D., Nakamura, A., Waltham, M. C., Gillespie, M. T. & Thompson, E. W. (2005) *Cancer Res.* **65,** 4929–4938.
36. Lee, S. E., Chung, W. J., Kwak, H. B., Chung, C. H., Kwack, K. B., Lee, Z. H. & Kim, H. H. (2001) *J. Biol. Chem.* **276,** 49343–49349.
37. Bezzi, M., Hasmim, M., Bieler, G., Dormond, O. & Ruegg, C. (2003) *J. Biol. Chem.* **278,** 43603–43614.
38. Xu, W., Mimnaugh, E., Rosser, M. F., Nicchitta, C., Marcu, M., Yarden, Y. & Neckers, L. (2001) *J. Biol. Chem.* **276,** 3702–3708.